ICSV 21
13-17 July, 2014, Beijing/China

The 21st International Congress on Sound and Vibration

13-17 July, 2014, Beijing/China

A LIMIT CYCLE FOR PRESSURE OSCILLATIONS IN A GAS TURBINE BURNER

Dmytro Iurashev[1], Andrea Di Vita[2], Ezio Cosatto[2], Giovanni Campa[2], Federico Daccà[2], Alessandro Bottaro[1]

[1]*University of Genoa, DICCA, via Montallegro 1, 16145 Genoa, Italy,*
[2]*Ansaldo Energia, PDE-ISV-TFC, via N. Lorenzi 8, 16152 Genoa, Italy,*
e-mail: dmytro.iurashev@edu.unige.it

Humming is a dangerous, combustion-driven acoustic oscillation phenomenon which can take place in gas-turbine burners. Any satisfactory description of humming should include both acoustic- and convective-related events. In fact, the distance crossed by a fluid "particle" during one humming period is typically of the same order of the distance between the flame and the inlet of the air-fuel mixture. Available models often postulate the Mach number to vanish, which is a scarcely justifiable hypothesis. Furthermore, the combined effect of non-normality and non-linearity might invalidate the familiar correspondence between humming onset and the growth rate of the humming mode predicted by linear stability theory. The prediction of humming amplitude, not available from linear theory, is required in order to assess the impact of the phenomenon. Thus, a non-linear – albeit simplified – description is required. We make use of a proprietary Ansaldo Energia model implemented in COMSOL Multiphysics, a finite element commercial software. Nonlinear terms are introduced into the heat release model and simulations are performed in the time domain. The initial condition in the simulations is composed by a set of random frequencies. The employed model filters both the fundamental frequency, the harmonics and the convective frequency from the initial signal; the variables in the model, such as pressure, velocity and temperature perturbations, oscillate in time without further application of external forces. The evolution scenarios of the pressure perturbation depend on the flame position and the mean velocity distribution. Three possible occurrences are observed: amplitude growth, decay and saturation.

1. Introduction

Combustion instabilities generally refer to the sustained high-amplitude pressure fluctuations of acoustic nature in a chamber where unsteady combustion takes place. It is essentially a self-excited oscillation, involving a complex interplay among unsteady heat release, acoustic fluctuation and vorticity field. Combustion instabilities represent a serious problem for combustion-driven devices, such as gas turbine engines and domestic burners. These instabilities can cause intense pressure oscillations, which in turn cause excessive structural vibrations, fatigue and even catastrophic damage to combustor hardware. In recent years, the development of clean combustion systems with reduced pollution of the environment has become a priority; however, such systems are particularly prone to combustion instabilities. There is an urgent need to understand the physical processes that are responsible so that methods to predict and prevent these instabilities should be developed.

Since combustion instabilities arise from the interaction among heat release fluctuations, pressure fluctuations and fuel/air modulation, the main point in the understanding of these instabilities is the behavior of the flame. The flame model developed by Crocco [1, 2] has been extensively adopted in the years by a large part of the literature. In this model heat release fluctuations are coupled to velocity fluctuations at the injection point through a parameter n and a time delay τ. In the original version by Crocco, this correlation was linear and several studies have been carried out in the years with this assumption [3], providing the stability behavior of the different systems investigated, as well as useful sensitivity analysis both in the frequency [4, 5, 6] and in the time domain [7]. However, the need to move to a nonlinear correlation between heat release fluctuations and velocity fluctuations has arisen lately, together with the increase of computational resources. Nonlinear analysis is able to provide additional information about the state of the system at different levels of amplitude and about the possibility to reach a limit cycle [8, 9, 10]. The importance of including the mean flow was shown by Nicoud and Wieczorek [11], thus it has to be taken into account.

In this paper a novel flame model is described and applied to a very simple configuration in a finite element method framework. The flame model is characterized by the presence of nonlinearities in air molar fraction and heat release perturbations, as previously illustrated by Di Vita et al. [12]. The aim of this paper is to show that the nonlinearities introduced are able to model the onset of a limit cycle.

The paper is organized as follows. First the mathematical model is introduced and the novel flame model used here is explained. Then, the configuration of study is described. Eventually, the results of simulations of four representative test cases are presented and discussed.

2. Mathematical model

In order to perform thermoacoustic studies, the conservation equations are written in the weak form. In this way it is possible to identify a function through its behavior with respect to a known test function, rather than knowing its values at given points. As soon as entropy waves can play a significant role in combustion instabilities [13, 14], perturbations of entropy have to be considered. For a viscous, compressible, Newtonian fluid, including the mean flow and assuming the fluid to be isotropic, the conservation equations of mass, momentum and energy are

$$\frac{D\rho}{Dt} + \rho\nabla\cdot\mathbf{u} = \frac{\partial\rho}{\partial t} + \nabla\cdot(\rho\mathbf{u}) = 0, \tag{1}$$

$$\rho\frac{D\mathbf{u}}{Dt} = \nabla\cdot\Big[-p\mathbf{I} + \mu_0(\nabla\mathbf{u} + \nabla\mathbf{u}^T) + (\mu_B - \frac{2}{3}\mu_0)(\nabla\cdot\mathbf{u})\mathbf{I}\Big], \tag{2}$$

$$\rho T\frac{DS}{Dt} = \rho T\Big[\Big(\frac{\partial S}{\partial T}\Big)_p\frac{DT}{Dt} + \Big(\frac{\partial S}{\partial p}\Big)_T\frac{Dp}{Dt}\Big] = q + \nabla\cdot(K\nabla T) + \phi, \tag{3}$$

where ρ is density, t is time, $\mathbf{u}$ is velocity vector, p is pressure, $\mathbf{I}$ is the identity matrix, μ_0 is viscosity, μ_B is bulk viscosity, T is temperature, S is entropy, q is heat release, K is thermal conductivity and ϕ is the viscous dissipation function. Partial derivative of entropy with respect to pressure at constant temperature and partial derivative of entropy with respect to temperature with constant pressure can be defined as

$$\Big(\frac{\partial S}{\partial p}\Big)_T = -\Big(\frac{\partial V}{\partial T}\Big)_p = -\Big[\frac{\partial}{\partial T}\Big(\frac{1}{\rho}\Big)\Big]_p = \frac{1}{\rho^2}\Big(\frac{\partial\rho}{\partial T}\Big)_p = -\frac{\alpha}{\rho}, \tag{4}$$

$$\Big(\frac{\partial S}{\partial T}\Big)_p = \frac{c_p}{T}, \tag{5}$$

where V is volume, α is the coefficient of thermal expansion and c_p is heat capacity at constant pressure. Introducing Eq. (4) and (5) into Eq. (3), the conservation of energy becomes

$$\rho c_p \frac{DT}{Dt} - \alpha T \frac{Dp}{Dt} = q + \nabla \cdot (K \nabla T) + \phi. \tag{6}$$

2.1 Linearization of equations

Considering each variable as a composition of a steady uniform part plus a small perturbation such as:

$$p(\mathbf{x}, t) = \bar{p} + p'(\mathbf{x}, t), \tag{7}$$

the linearized equations for the perturbations are obtained for the conservation equations

$$\frac{\partial \rho'}{\partial t} + \nabla \cdot \rho' \bar{\mathbf{u}} + \nabla \cdot \bar{\rho} \mathbf{u}' = 0, \tag{8}$$

$$\bar{\rho} \left[\frac{\partial \mathbf{u}'}{\partial t} + \bar{\mathbf{u}} \cdot \nabla \mathbf{u}' + \mathbf{u}' \cdot \nabla \bar{\mathbf{u}} \right] + \rho' \bar{\mathbf{u}} \cdot \nabla \bar{\mathbf{u}} = \nabla \cdot \left[-p' \mathbf{I} + \mu_0 \left(\nabla \mathbf{u}' + \nabla \mathbf{u}'^T \right) + (\mu_B - \frac{2}{3} \mu_0) \nabla \cdot \mathbf{u}' \mathbf{I} \right], \tag{9}$$

$$\begin{aligned} &\rho' c_p \bar{\mathbf{u}} \cdot \nabla \bar{T} + \bar{\rho} c_p \left[\tfrac{\partial T'}{\partial t} + \bar{\mathbf{u}} \cdot \nabla T' + \mathbf{u}' \cdot \nabla \bar{T} \right] - \\ &- \alpha T' \bar{\mathbf{u}} \cdot \nabla \bar{p} - \alpha \bar{T} \left[\tfrac{\partial p'}{\partial t} + \bar{\mathbf{u}} \cdot \nabla p' + \mathbf{u}' \cdot \nabla \bar{p} \right] = \nabla \cdot K \nabla T' + q' + \phi_{10} \,, \end{aligned} \tag{10}$$

under the assumption that μ_0, μ_B, c_p, α and K are constant in time and depend only on value of the mean temperature. The viscous dissipation function ϕ_{10} is defined as follows

$$\begin{aligned} \phi_{10} = &\nabla \mathbf{u}' : \left[\mu_0 \left(\nabla \bar{\mathbf{u}} + \nabla \bar{\mathbf{u}}^T \right) + \left(\mu_B - \tfrac{2}{3} \mu_0 \right) \nabla \cdot \bar{\mathbf{u}} \mathbf{I} \right] + \\ &+ \nabla \bar{\mathbf{u}} : \left[\mu_0 \left(\nabla \mathbf{u}' + \nabla \mathbf{u}'^T \right) + \left(\mu_B - \tfrac{2}{3} \mu_0 \right) \nabla \cdot \mathbf{u}' \mathbf{I} \right]. \end{aligned} \tag{11}$$

The system of equations (8)-(10) consists from 5 equations with 6 unknown variables. The closing equation is the equation of state:

$$\rho' = p' \left(\frac{\partial \rho}{\partial p} \right)_{\bar{T}} + T' \left(\frac{\partial \rho}{\partial T} \right)_{\bar{p}} = \bar{\rho} \left(p' \beta_T - T' \alpha \right), \tag{12}$$

where β_T is a coefficient of compressibility. Due to its simplicity, the state equation is set in algebraic form rather than in the weak form to limit the matrices size and to lighten computation.

2.2 Heat release model

The present, analytical model has been originally developed in Ansaldo Energia [12] in order to investigate limit cycles. For simplicity, the lean combustion of a perfectly premixed mixture of air and fuel is considered. Mach number is supposed to be far from one and total pressure is the same everywhere. The flame is assumed to be a thin layer with constant thickness δ_f which separates regions with burnt and not-yet-burnt gases, so that combustion occurs only at the flame. Mean temperature is assumed constant and uniform with a gradient across the flame.For simplicity, the flame is supposed to be axisymmetric. This flame model leads to a limit cycle by introducing just one more variable: the air molar fraction z, defined as

$$z = \frac{n_{air}}{n_{air} + n_{fuel}}, \tag{13}$$

where n_{air} is the amount of air and n_{fuel} is the amount of fuel.

The inlet fuel pressure is assumed to be constant, so that air molar fraction at the inlet depends only on pressure perturbations of air and is estimated as

$$z_{inlet} = \frac{n_{air}}{n_{air} + n_{fuel}} = \frac{\frac{\bar{p}_{air}+p'}{RT}}{\frac{\bar{p}_{air}+p'}{RT} + \frac{\bar{p}_{fuel}}{RT}} = 1 - \frac{\bar{p}_{fuel}}{\bar{p}_{air} + \bar{p}_{fuel} + p'}. \tag{14}$$

The air molar fraction oscillations are convected from the inlet to the flame, according to:

$$\frac{\partial z}{\partial t} + (\bar{\mathbf{u}} + \mathbf{u}') \cdot \nabla z = 0. \tag{15}$$

The feedback mechanism is closed by connecting air molar fraction at the flame and heat release perturbations through variations in the flame velocity v_f, i.e.

$$v_f = v_{fM} \frac{z^{1+C_1}(1-z)^{1+C_2}}{\left(\frac{1+C_1}{2+C_1+C_2}\right)^{1+C_1}\left(1-\frac{1+C_1}{2+C_1+C_2}\right)^{1+C_2}}, \tag{16}$$

where $C_1 = 14.53$ and $C_2 = 0.553$ are constants and chosen in such a way that

- the flame velocity v_f is equal to its maximum value v_{fM} when the reaction is stoichiometric ($z_{stoichiometric} = 10/11$ for methane and air);
- in the limit cases of no air ($z = 0$) and no fuel ($z = 1$) the flame speed vanishes.

Fig. 1 displays the dependence of the flame velocity v_f on air molar fraction z with the coefficients mentioned.

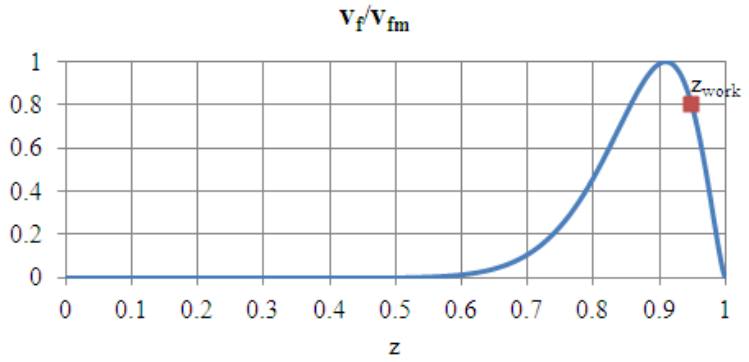

Figure 1. Flame velocity as a function of air molar fraction

Finally, the oscillating heat release is linearized around the "working" condition

$$q' = \frac{H}{\delta_f}\rho Y\Big(v_f(z) - v_f(z_{work})\Big), \tag{17}$$

where H is a higher heating value, Y is the fuel mass fraction and z_{work} is the base value, defined as

$$z_{work} = \frac{\bar{p}_{air}}{\bar{p}_{air} + \bar{p}_{fuel}}. \tag{18}$$

We consider that an oscillating heat source produces pressure perturbations that eventually reach the inlet. Partial differential equations (8)-(10) and (15) are solved in a Finite Element Method framework. Definitions of viscous dissipation function in Eq. (11), flame velocity in Eq. (16), heat release perturbations in Eq. (17) and the boundary condition for air molar fraction in Eq. (14) are also introduced in the system to be solved.

3. Description of the configuration

The configuration is a 300 mm long one-dimensional (1D) duct with constant cross-section and the flame positioned at 100 mm from the inlet (Fig. 2). The flame is considered to be a flat sheet (and in this 1D configuration it degenerates into a point) and the flame thickness δ_f is assumed to be equal to 1 mm. There is no movement of the flame and the setup is assumed to be adiabatic. The operating pressure $\bar{p}$ is uniform along the tube and is equal to 18.4 bar; the mean temperature is equal to 661 K before the flame and 1200 K after the flame.

The base value of air molar fraction for each test case in this paper is taken equal to $z_{work} = 0.947$. The maximum flame velocity v_{fM} is calculated in such a way that for the base value of air molar fraction, the flame velocity is equal to the mean velocity before the flame.

Two types of acoustical boundary conditions are employed: acoustically closed ($u' = 0$) and acoustically open ($p' = 0$). Temperature perturbations are set to be equal to zero ($T' = 0$) at the inlet. Despite entropy waves are considered in the implemented equations, their interaction with acoustic waves is not taken into account by corresponding boundary conditions.

The configuration has uniform computational mesh with mesh size equal to 0.5 mm. Time step is calculated taking the Courant number to be equal to 0.1, which yields reliable solutions.

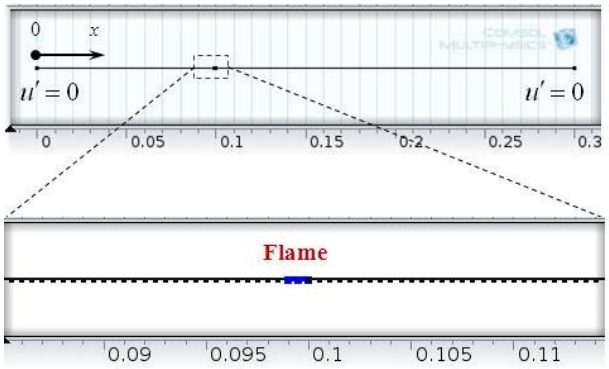

Figure 2. 30-cm configuration

We impose our initial signal setting values of air molar fraction between the inlet and the flame different from the base value. The initial signal is represented by the sum of 200 sine waves with both random frequency (in the range of 10Hz and 5kHz), amplitude and phase. The Fast Fourier Transform of one such signals is shown in Fig. 3.

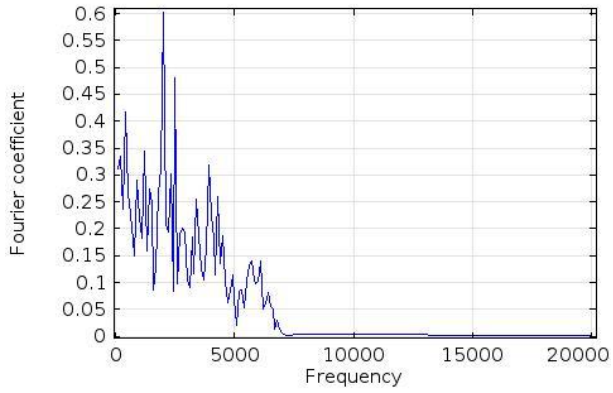

Figure 3. Fast Fourier Transform of initial random signal

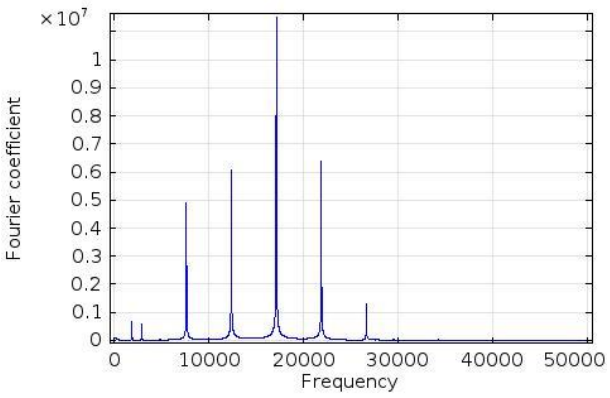

Figure 4. Fast Fourier Transform of the pressure perturbations. Test case 1. The acoustic frequency corresponds to 1 kHz

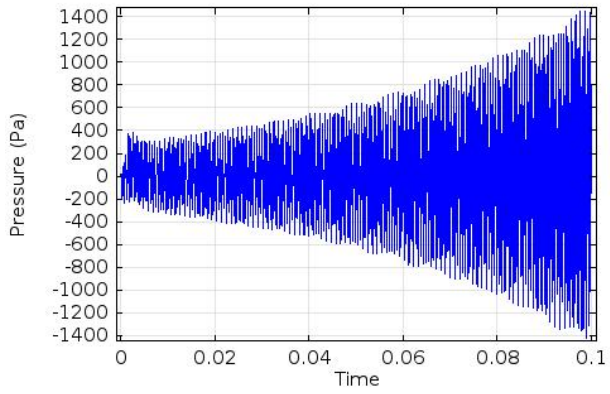

Figure 5. Pressure perturbations. Test case 2

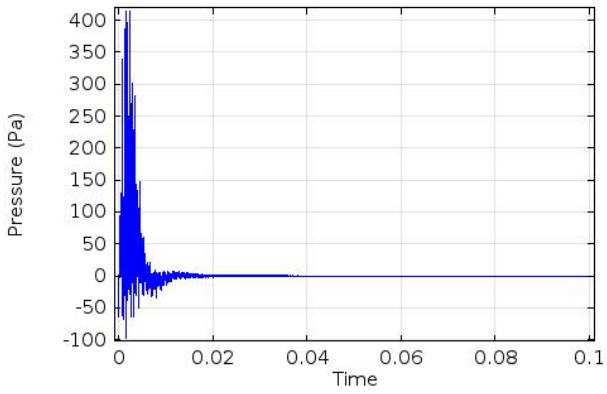

Figure 6. Pressure perturbations. Test case 3

4. Results and discussion

4.1 Test case 1. Filtering

In the first case the value of the mean velocity before the flame has been set to 98 m/s. Such a high value has been chosen in order to get more visible spectrum of frequencies of the pressure oscillations in the same computational time. After the flame the value of mean velocity satisfies conservation of mass, assuming that the duct has uniform cross-section. Acoustically closed boundary conditions ($u' = 0$) at both the inlet and the outlet have been employed in this test case.

The results of simulations show us that the employed model, described in Section 2, works like a filter and, after a period of transient, we observe only convective and acoustic frequencies (Fig. 4). Given the small length of the configuration, the value of the fundamental frequency is about 1 kHz. Also the range of frequencies in Figs. 3-4 is wide and is up to 50 kHz. It can be observed that, whatever is the random input signal, the FFT of the pressure perturbations provides only the fundamental frequency and its harmonics.

4.2 Test cases 2 and 3. Growth and decay

Test cases 2 and 3 refer to the same configuration, except for the value of the mean velocity, which is set to 65 m/s and to 55 m/s, respectively. Acoustically closed boundary conditions ($u' = 0$) at both the inlet and the outlet were employed in these test cases. The results of the simulations, which are displayed in Fig. 5 and Fig. 6, indicate two different behaviors. Fig. 5 shows that, in test case 2 with $\bar{u} = 65$ m/s, a growth of the amplitude of pressure perturbations occurs. On the other hand, Fig. 6 shows that with another value of the mean velocity pressure perturbations are damped.

4.3 Test case 4. Limit cycle

In test case 4 the boundary conditions are changed: acoustically closed ($u' = 0$) inlet and acoustically open ($p' = 0$) outlet are considered. The value of the mean velocity between inlet and the flame is equal to 34 m/s. Pressure perturbations at the flame for this configuration are shown in Fig. 7: after an initial exponential growth the pressure disturbance reaches a limit cycle. Saturation is due to the presence of nonlinearities in the heat release model, cf. Eqs. (14) and (16), coupled to the boundary and operating conditions adopted in this configuration.

5. Conclusions

It has been shown that the model employed filters fundamental acoustic frequency and harmonics from a generic initially random signal. For different values of unperturbed velocity we can observe

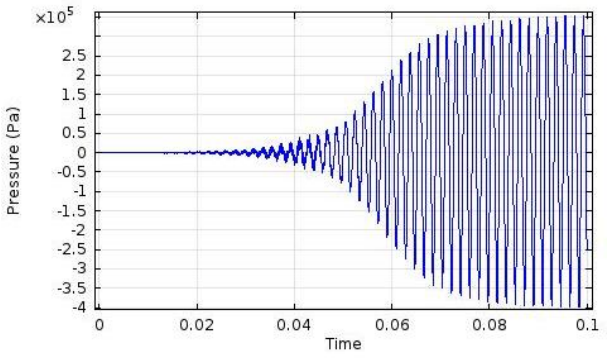

Figure 7. Pressure perturbations. Test case 4

either growth or decay of the amplitude of pressure perturbations. Moreover, it has been shown that nonlinearities introduced in the model also permit pressure oscillations to saturate to the limit cycle.

Moreover, the model employed considers the presence of entropy waves, but does not yet takes into account interaction between them and acoustic waves. As it has been shown by Polifke et al. [13] and Hochgreb et al. [14], this interaction could be crucial and it has to be introduced into the model. This is the subject of current work.

6. Acknowledgements

This work is part of the Marie Curie Initial Training Network Thermo-acoustic and aero-acoustic nonlinearities in green combustors with orifice structures (TANGO). We gratefully acknowledge the financial support from the European Commission under call FP7-PEOPLE-ITN-2012.

REFERENCES

[1] Crocco, L. Aspects of combustion instability in liquid propellant rocket motors. part i. J. *American Rocket Society* **21**, 163–178, (1951).

[2] Crocco, L. Aspects of combustion instability in liquid propellant rocket motors. part ii. J. *American Rocket Society* **22**, 7–16, (1952).

[3] Culick, F.E.C., *Unsteady Motions in Combustion Chambers for Propulsion Systems*. RTO AGAR-Dograph, AG-AVT-039, (2006).

[4] Dowling, A.P., Stow, S.R. Acoustic Analysis of Gas Turbine Combustors, *Journal of Propulsion and Power*, **19** (5), 751–764, (2003).

[5] Camporeale, S.M., Fortunato, B., Campa, G. A Finite Element Method for Three-Dimensional Analysis of Thermoacoustic Combustion Instability, *Journal of Engineering for Gas Turbines and Power*, **133** (1), 011506, (2011).

[6] Sensiau, C., Nicoud, F., Poinsot, T. A tool to study azimuthal standing and spinning modes in annular combustors. *International Journal of Aeroacoustics*, **8** (1), 57–67, (2009).

[7] Pankiewitz, C., Sattelmayer, T. Time Domain Simulation of Combustion Instabilities in Annular Combustors. *Journal of Engineering for Gas Turbines and Power*, **123** (3), 677–685, (2003).

[8] Balasubramanian, K., Sujith, R. I. Thermoacoustic instability in a Rijke tube: Non-normality and nonlinearity. *Physics of Fluids* **20**, 044103 (2008).

[9] Balasubramanian, K., Sujith, R. I. Non-normality and nonlinearity in combustion–acoustic interaction in diffusion flames. *J. Fluid Mech.*, **594**, 29–57 (2008).

[10] Heckl, M.A. Analytical model of nonlinear thermo-acoustic effects in a matrix burner. *Journal of Sound and Vibration*, **332**, 4021–4036, (2013).

[11] Nicoud, F., Wieczorek, K. About the zero Mach assumption in the calculation of thermoacoustic instabilities. *International journal of spray and combustion dynamics*, **1**, 67-112, (2009).

[12] Di Vita, A., Baccino, F., Cosatto, E. A limit cycle for pressure oscillations in a premix burner. *AIA-DAGA 2013. Conference on Acoustics. EAA Euroregio - EAA Winter School*. Merano, Italy, 18-21 March (2013).

[13] Polifke, W., Paschereit, C.O., Dobbeling, K. Constructive and Destructive Interference of Acoustic and Entropy Waves in a Premixed Combustor with a Choked Exit. *International Journal of Acoustics and Vibration*, **6** (3), (2001).

[14] Hochgreb, S., Dennis, D., Ayranci, I., Bainbridge, W., Cant, S., Forced and self-excited instabilities from lean premixed, liquid-fuelled aeroengine injectors at high pressures and temperatures. *Proceedings of ASME Turbo Expo 2013: Turbine Technical Conference and Exposition*, San Antonio, Texas, USA, 3-7 June, (2013).

[15] Baccino, F. *On the onset of limit cycles in models of Ansaldo's gas turbine burners*, Master of Science Thesis, University of Genova, (2013)